# Vacuum-Deposited Planar Heterojunction Polymer Solar Cells

**Peter Kovacik,*,† Giuseppe Sforazzini,†,‡ Andrew G. Cook,† Shawn M. Willis,† Patrick S. Grant,† Hazel E. Assender,† and Andrew A. R. Watt*,†**

Department of Materials, University of Oxford, Parks Road, OX1 3PH Oxford, United Kingdom, and Department of Chemistry, University of Oxford, 12 Mansfield Road, OX1 3TA Oxford, United Kingdom

**ABSTRACT** The vacuum thermal evaporation of poly(3-hexylthiophene) (P3HT) for application in photovoltaic cells is demonstrated. Structural changes before and after evaporation are determined using GPC, UV−vis absorption spectroscopy, NMR, and FTIR. GPC showed that the polymer molecular weight is reduced during evaporation, leading to a blue-shift of the absorption spectra. FTIR and NMR were used to examine the change in chemical structure: it was found that conjugation remains mostly intact; however, the conjugation length decreases and side chains dissociate from the backbone. Bilayer heterojunction solar cells were fabricated by sequential deposition of P3HT and $C_{60}$ and the photovoltaic response measured.

**KEYWORDS:** organic solar cells • conjugated polymers • poly(3-hexylthiophene) • vacuum thermal deposition • thin films

## INTRODUCTION

Electronic products based on organic thin film semiconductors have a plethora of applications that take advantage of the mechanical flexibility and the ability to manufacture on a large scale at low cost. Roll-to-roll (R2R) processing of conjugated polymers has largely focused upon solution-based printing and coating (1). Vacuum processing of materials has several advantages such as parallel and sequential deposition (2); however the deposition of conjugated polymers under these conditions is a challenge. This paper presents a simple method for the thermal deposition of poly(3-hexylthiophene) (P3HT), examines how chemical properties are modified on deposition, and demonstrates photovoltaic devices based on vacuum-deposited P3HT/$C_{60}$.

Organic semiconductors used in solar cells fall into two main groups: low-molecular-weight "molecular" materials that are usually vacuum deposited, and higher-molecular-weight polymers which are usually solution processed. Polymer photovoltaics take advantage of the freedom of chemical design to produce efficient light absorbers and electron-donors for use in heterojunction structures with fullerene derivatives (3). The most prolific polymer for photovoltaics is poly(3-hexylthiophene) because of its enhanced hole-transport properties that when blended with PCBM have lead to some of the highest-efficiency polymer devices (4, 5).

As in the case of inorganic photovoltaics, the best performing device architectures use multilayered structures (6). The choice of deposition technique is, therefore, pivotal to the final cell performance (7). Solution processing of sequential organic thin films can be limited as the use of nonorthogonal solvents can damage the previously deposited layers (8). This substantially limits the complexity of the devices that can be obtained using solvent based methods. Vacuum thermal deposition is another common way of processing thin films and is already well-established in surface science and coating industry (9). Moreover, energy requirements for this technique are comparable to those needed for solution-based coating and printing of an active layer (when costs of solvents and $N_2$ atmosphere are considered) (10). If vacuum deposition can be applied to polymers, it would have the following advantages over solution processing: absence of solvents allows for two or more materials to be easily codeposited, an unlimited number of layers can be deposited on top of each other, layer thickness can be controlled with nanometer precision, absence of solvents minimizes negative environmental impact, vacuum processing reduces number of impurities (11), overall device production costs can be lowered by conducting all of the process steps in the same environment (electrodes as well as active layer).

However, the process puts constraints on the thermal stability of the organic molecules. In particular, heating of polymers to high temperatures generally results in a decrease in molecular weight and even changes to local chemistry (12, 13). In organic field-effect transistors, thermally deposited polymers have been used for the insulator layers (14–16). Structural analysis of a thermally evaporated organic semiconductor was recently reported by Wei et al. (17), who successfully demonstrated that P3HT can withstand such treatment while largely retaining its chemical composition. This opens up the potential to thermally deposit conjugated polymers for organic electronics.

* Corresponding author. E-mail: peter.kovacik@materials.ox.ac.uk (P.K.); andrew.watt@materials.ox.ac.uk (A.A.R.W.). Phone: +44 (0)1865 613455.
Received for review March 24, 2010 and accepted November 24, 2010
† Department of Materials, University of Oxford.
‡ Department of Chemistry, University of Oxford.
DOI: 10.1021/am1008985




ARTICLE

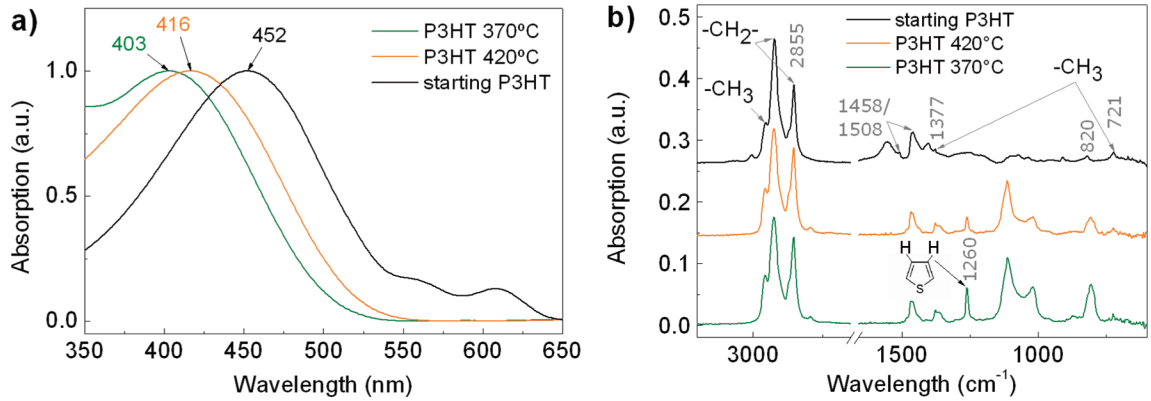


**FIGURE 1. (a) UV−vis absorption spectra of P3HT evaporated at 370 and 420 °C in comparison with the starting material. The absorption peaks are normalized to the highest intensity. (b) FT-IR spectra of starting P3HT and P3HT after evaporation at 370 and 420 °C.**

## EXPERIMENTAL METHODS

Photovoltaic devices were prepared by sequentially thermally evaporating P3HT and $C_{60}$ in between an Al cathode and an ITO-on-glass anode as follows. The ITO surface was cleaned with acetone and isopropanol and then treated with oxygen plasma for 10 s. A layer of conducting polymer poly(3,4-ethylenedioxythiophene)-poly(styrenesulfonate) (PEDOT:PSS, Baytron P dispersion, H.C. Starck) was spin coated at 5000 rpm for 30 s onto the prepared ITO surface and then heated for 5 min at 140 °C. Next, a layer of 90% regioregular poly(3-hexylthiophene) (P3HT, Rieke Metals) and a layer of fullerene ($C_{60}$, 99.9% pure, MER Corporation) were sequentially deposited onto the substrate by thermal evaporation in high vacuum (~$1 \times 10^{-5}$ Torr). The evaporation was done by heating a tungsten boat (Leybold Optics) using a Xantrex XHR 7.5−80 DC Power Supply. The boat temperature was measured using a K-type exposed thermocouple mounted inside the boat. P3HT was deposited at a temperature of 360 ± 5 °C at a rate of ~1 nm/min and $C_{60}$ at the rate of ~2 nm/min. The layer thickness was controlled in situ using a quartz crystal microbalance (Q-Pod, Inficon) placed at the same distance from the source as the substrates. After the deposition, the value was further verified by Veeco DEKTAK surface profiler (Dektak 6 M Stylus Profiler). Finally, a set of 90 nm thick Al electrodes was evaporated on top of the sandwich structure. Photovoltaic characterization of the devices was carried out under white light illumination (AM1.5, 80 mW/cm$^2$) in an inert $N_2$ atmosphere. A set of neutral OD filters (Melles Griot) were used for varying the illumination intensity. Current−voltage characteristics were measured using a Keithley 2400 source measurement unit.

The surface morphology of the thin films was imaged by MircoXAM surface mapping microscope (ADE phase Shift). A UV−vis−NIR spectrophotometer Cary 5000 was used to obtain optical absorption of the films. These measurements were performed in air, right after the vacuum deposition of materials on ITO-on-glass substrates. The UV−vis characterization of the starting P3HT and that evaporated at 370 ± 5 °C and 420 ± 5 °C was done in chloroform solution on the same spectrophotometer. Infrared spectra of the polymers were measured with an attenuated total reflectance extension on a Varian UMA-600 FT-IR spectrometer. The samples were dissolved in chloroform and cast onto the crystal window. NMR spectra were recorded on a Bruker DPX 400 MHz at 298K. GPC was carried out using PLgel mm Mixed-D columns (2 mm × 300 mm lengths, 7.5 mm diameter) from Polymer Laboratories calibrated with polystyrene narrow standards (Mp = 1300 to 11.2 × $10^6$ g/mol) in THF with toluene as flow marker, using UV (254 nm). The THF was degassed with helium and pumped at a rate of 1 mL/min at 30.0 °C.

## RESULTS AND DISCUSSION

Thermal behavior of P3HT was studied using differential scanning calorimetry (DSC) and ThermoGravimetric analysis (TGA) under an $N_2$ atmosphere at atmospheric pressure. DSC identified the glass-transition temperature to be 130 °C and the melting temperature to be 230 °C. This melting temperature corresponded well with that determined by differential thermal analysis: 227 °C. Both values are in agreement with previously published literature (18, 19). The mass loss of the polymer takes place at 400 °C and reaches a plateau of 28% at 510 °C, as measured by TGA.

To study the influence of temperature on the polymer structure, we performed chemical characterization on the following samples: P3HT before evaporation and P3HT evaporated at two different temperatures (370 and 420 °C). It was found from gel permeation chromatography (GPC) that the molecular weight ($M_w$) of the polymer was reduced during the thermal deposition process. The $M_w$ of P3HT decreased from 36 000 g mol$^{-1}$ to about 1500 g mol$^{-1}$ for both 370 and 420 °C. This lower molecular weight corresponds to a weight of an oligomer with approximately 9 monomeric units. The reduction in the average $M_W$ is in accordance with theoretical limitations on maximal molecular weight, which evaporated polymer fractions can retain during the evaporation process (12).

Light absorption of P3HT thin films depends on their molecular weight (20). UV−vis spectroscopy was therefore performed on all our samples and the spectra were compared, as shown in Figure 1a. The absorption peak of the evaporated polymer shifts to a blue region, with a maximum at 403 nm for 370 °C and 416 nm for 420 °C in comparison to 452 nm for the starting polymer. The blue shift indicating the molecular weight decrease is in good agreement with what has been observed previously for P3HT (20, 21). The results are also consistent with the $M_w$ loss measured by GPC.

Infrared spectroscopy (FTIR) and nuclear magnetic resonance (NMR) were used to investigate the chemical changes in the polymer structure. Figure 1b shows differences in FTIR spectra between starting and evaporated P3HT. The band assignments and the changes in intensity observed on thermal evaporation are summarized in Table 1. The bands

**Table 1. Summary of Band Assignments and Intensity Changes in the FTIR Spectra of P3HT**

| wavenumber | vibration | on evaporation |
|---|---|---|
| 721 | rocking vibrations of the methyl group $-CH_3$(17) | similar |
| 820 | aromatic C−H out-of-plane vibration | increased |
| 1015−1120 | oxidation(22) | increased |
| 1260 | in-plane C−H bending of the thiophene ring moieties(23) | increased |
| 1377 | deformation vibrations of the methyl group $-CH_3$(17) | similar |
| 1458 | symmetric ring stretching vibrations | similar |
| 1508 | asymmetric ring stretching vibrations | decreased |
| 2855 | symmetric C−H stretching vibrations of methylene $-CH_2-$ moieties (24, 25) | similar |
| 2926 | asymmetric C−H stretching vibrations of methylene $-CH_2-$ moieties (24, 25) | similar |
| 2957 | asymmetric C−H stretching of the methyl group $-CH_3$(17) | similar |
| 3055 | aromatic C−H stretching vibration | decreased |

at 1458 and 1508 $cm^{-1}$ are associated with symmetric and asymmetric ring stretching vibrations, respectively, and their relative ratio indicates the conjugation length of the polymer (26). In evaporated samples, the intensity of the absorption peak at 1508 $cm^{-1}$ appears to be reduced, which implies a reduction in the conjugation length inferred to be due to the decrease in molecular weight. The strong absorption at 1260 $cm^{-1}$ is assigned to in-plane C−H bending of the thiophene ring moieties (23) (and similarly changes in absorption at 820 and 3055 associated with C−H vibrations), suggesting either a loss of hexyl side chains or a decrease in conjugation. As the samples were prepared and characterized in air, the unavoidable oxidation might have modified the spectra by giving rise to additional absorption bands, e.g., those at 1015−1120 $cm^{-1}$ (22). Overall, it can be concluded from FTIR that the polymer undergoes several structural changes during the deposition process, the most pronounced being the decrease in conjugation length.

Structural studies by proton $^1H$ NMR showed similar results to those obtained from infrared spectroscopy (see the Supporting Information). The polymer retained its conjugated character, however several differences in the aromatic and alkyl signal regions were detected. Comparing the starting and evaporated P3HT in proton 1H NMR new bands appear at 7.3−8, 1.8−2.7 and 3−6 ppm. The first band implies an increase in the number of protons in the thiophene ring environment and thus a loss of the side chains or conjugation length (27). The latter two bands indicate the presence of various small moieties consisting of single and double carbon bonds that are most likely due to dissociation of some of the ring structures or oxidation products (22). Strengthening of the alkyl band at 1.3−1.4 ppm and the methyl band at 0.9 ppm could come from the symmetry of the proton environments within the alkyl chain (28). This could be caused by breaking of the side groups away from the backbone.

Figure 2a−d compares surface morphology of P3HT thin films (20, 35, and 50 nm) deposited directly onto the PEDOT:PSS electrode surface, a being a monolayer whereas each of b−d was covered with a 120 nm thick layer of $C_{60}$. As can be seen in Figure 2a, polymer aggregation caused by poor substrate wetting creates large variations in the film thickness. This topography leads to low shunt resistance of the active layer due to partial shorting across the device, and thus limited device performance. The effect is pronounced especially in polymer homojunctions and planar heterojunc-

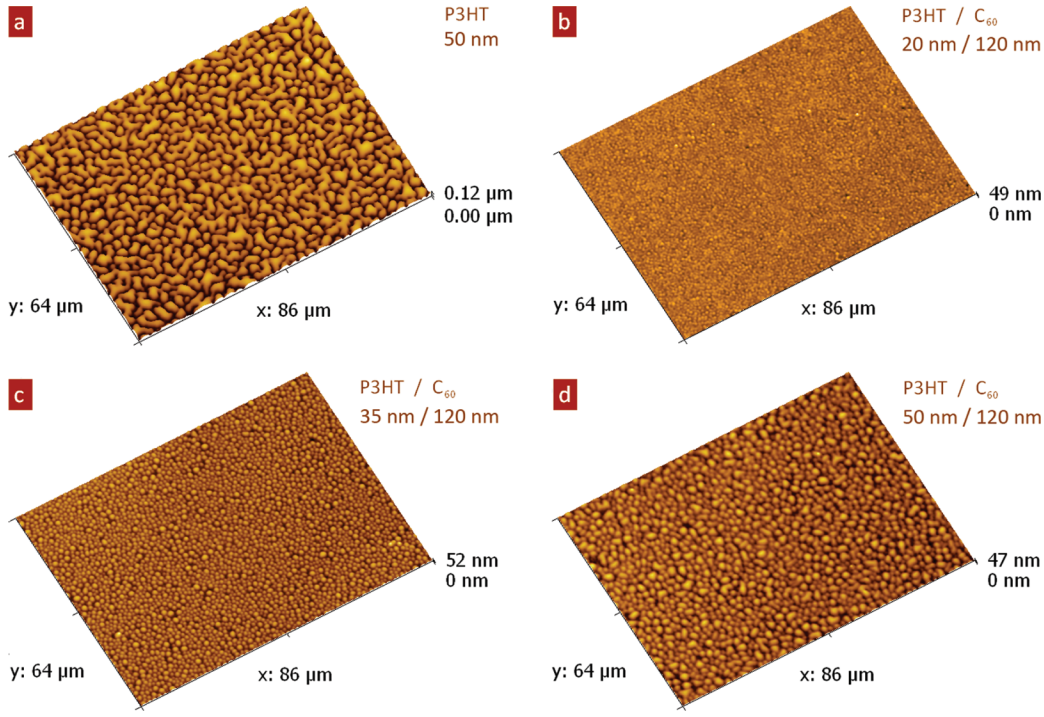


**FIGURE 2. (a) MicroXAM image of 50 nm thick P3HT film on PEDOT:PSS coated ITO substrate. (b−d) Surface morphology of 120 nm $C_{60}$ on P3HT with the thickness of (b) 20, (c) 35, and (d) 50 nm.**

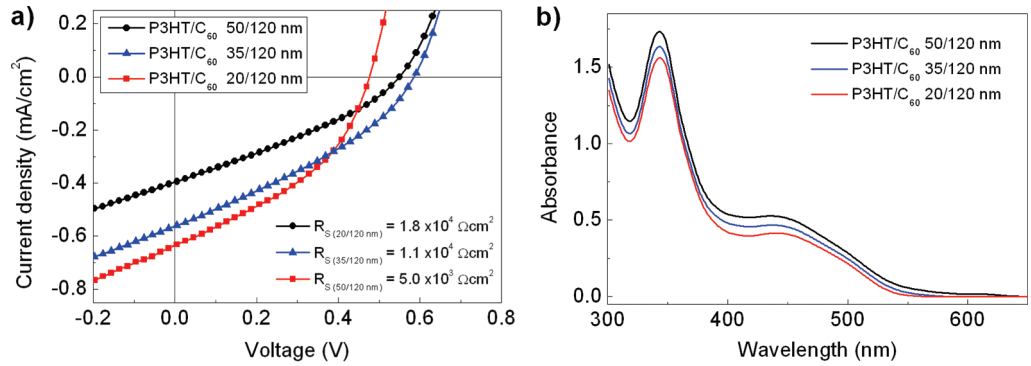


**FIGURE 3. (a) Current density−voltage characteristics of planar heterojunctions with different P3HT thicknesses (20, 35, and 50 nm) and 120 nm layer of $C_{60}$. Average power conversion efficiencies (PCE) and fill factors (FF) of the devices were as follows: $PCE_{50/120} = 0.08\%$ and $FF_{50/120} = 31.5\%$ (circles), $PCE_{35/120} = 0.13\%$ and $FF_{35/120} = 34.1\%$ (triangles), $PCE_{20/120} = 0.13\%$ and $FF_{20/120} = 38.0\%$ (squares). (b) Absorbance spectra of the P3HT/$C_{60}$ bilayers.**

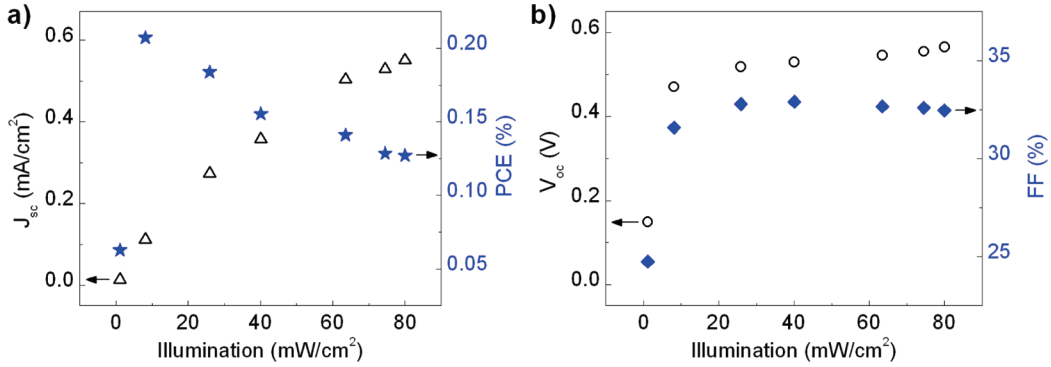


**FIGURE 4. (a) $J_{sc}$ (triangles) and PCE (stars) of the P3HT/$C_{60}$ 35/120 nm cell as a function of incident illumination intensity. (b) $V_{oc}$ (circles) and FF (diamonds) of the P3HT/$C_{60}$ 35/120 nm cell as a function of incident illumination intensity.**

tions with very thin P3HT layers (see Figure 3b below). Surface morphology of $C_{60}$ on P3HT with varying thickness is shown in Figure 2b−d. An increase in surface roughness is due to greater roughening of the underlying P3HT layer. While shallow pits in a 20 nm average thickness of P3HT are largely filled in by the 120 nm of $C_{60}$ on top, the pits of thicker P3HT layers get deeper and hence are reflected in the $C_{60}$ surface topography.

To demonstrate the capabilities of the vacuum thermal deposition of conjugated polymers, we fabricated a series of P3HT/$C_{60}$ planar heterojunction solar cells and measured their photovoltaic response. Figure 3a shows $J-V$ characteristics of the devices as a function of P3HT thickness (20, 35, and 50 nm, the $C_{60}$ always had thickness of 120 nm). Although the absorbance of the cells increases with increasing thickness of the donor layer (cf. Figure 3b), the value of $J_{SC}$ and FF decreases with increasing thickness of the donor layer. This decrease in charge collection efficiency can result from the larger distance necessary for hole collection and from the low exciton diffusion length in P3HT (29). Series resistance ($R_s$) was calculated using the diode equation (30) as an inverse value of the $J-V$ curve slope at $J = 0$ mA/cm$^2$. $R_s$ was found to be of the order of $1 \times 10^3$ to $1 \times 10^4$ Ωcm$^2$, where larger $R_s$ corresponds to thicker P3HT. Consistently we see that thinner P3HT films result in lower $V_{oc}$ (see the Supporting Information). This we attribute to the morphology of P3HT on the PEDOT:PSS surface discussed earlier. Power conversion efficiency (PCE) of the cells is comparable to that of spin-coated P3HT/$C_{60}$ planar heterojunctions previously reported in literature ($PCE_{evaporated\ 35/120\ nm} = 0.13\%$ vs $PCE_{solution\text{-}processed\ 30/200\ nm} = 0.17\%$) (31). Of course, rather higher efficiencies might be expected from a codeposited bulk heterojunction structure.

The effect of illumination intensity was measured on one of the well-performing cells (P3HT/$C_{60}$ 35/120 nm) and is shown in Figure 4a,b. Although $V_{oc}$ and FF remain relatively constant down to 8 mW/cm$^2$, $J_{sc}$ increases nonlinearly as the illumination is reduced. As a result, the PCE of the cells increases to a maximum of 0.21% at 8 mW/cm$^2$. Lower device performance at illuminations above 8 mW/cm$^2$ can result from limited absorption of the thin P3HT films. To improve on this, we are developing thicker and more optically dense bulk heterojunction as well as stacked/tandem architectures using the evaporation technique.

## CONCLUSION

We have investigated the vacuum thermal deposition of P3HT and successfully applied it to the production of planar heterojunction photovoltaic cells. Structural studies of the polymer before and after evaporation revealed structural changes upon thermal evaporation. The most pronounced change is the loss of molecular weight and cleavage of the alkyl side chains from the conjugated backbone. Topological characterization of the vacuum deposited thin films showed that P3HT dewets and forms island structures. The underlying roughness of P3HT layers was reflected in roughening of the P3HT/$C_{60}$ bilayers. Finally, planar heterojunction solar cells with different P3HT thickness were fabricated as a

demonstration of the deposition method. The photovoltaic response of devices underlines the potential to fabricate complex multilayered structures with enhanced performance. Although vacuum thermal deposition of conjugated polymers appears to be a promising alternative to coating and printing methods, further work needs to be done especially in the field of polymer chemical design. Application of less bulky and more thermally stable materials as well as codeposition of bulk heterojunction devices are currently under investigation. Blended films made by parallel deposition of two materials may not suffer from poor wetting and performance of such architecture should be significantly better than that of the planar.

**Acknowledgment.** The authors are grateful to Mr Richard Turner for assistance with the TGA measurements, and to EPSRC and John Fell Fund for financial support.

**Supporting Information Available:** $^1$H NMR spectra of the starting and evaporated P3HT, dependence of $V_{oc}$ of P3HT/$C_{60}$ bilayer on the P3HT thickness (PDF). This material is available free of charge via the Internet at http://pubs.acs.org.

## REFERENCES AND NOTES

(1) Krebs, F. C. *Sol. Energy Mater. Sol. Cells* **2009**, *93* (4), 394–412.
(2) Xue, J. G.; Uchida, S.; Rand, B. P.; Forrest, S. R. *Appl. Phys. Lett.* **2004**, *84* (16), 3013–3015.
(3) Scharber, M. C.; Wuhlbacher, D.; Koppe, M.; Denk, P.; Waldauf, C.; Heeger, A. J.; Brabec, C. L. *Adv. Mater.* **2006**, *18* (6), 789.
(4) Ma, W. L.; Yang, C. Y.; Gong, X.; Lee, K.; Heeger, A. J. *Adv. Funct. Mater.* **2005**, *15* (10), 1617–1622.
(5) Kim, J. Y.; Lee, K.; Coates, N. E.; Moses, D.; Nguyen, T. Q.; Dante, M.; Heeger, A. J. *Science* **2007**, *317* (5835), 222–225.
(6) Devos, A. *J. Phys. D: Appl. Phys.* **1980**, *13* (5), 839–846.
(7) Dennler, G.; Scharber, M. C.; Brabec, C. J. *Adv. Mater.* **2009**, *21* (13), 1323–1338.
(8) Forrest, S. R. *Nature* **2004**, *428* (6986), 911–918.
(9) Bishop, C. *Vacuum Deposition Onto Webs, Films and Foils*; William Andrew: Norwich, NY, 2007.
(10) Garcia-Valverde, R.; Miguel, C.; Martinez-Bejar, R.; Urbina, A. *Solar Energy* **2009**, *83* (9), 1434–1445.
(11) Welte, L.; Garcia-Couceiro, U.; Castillo, O.; Olea, D.; Polop, C.; Guijarro, A.; Luque, A.; Gomez-Rodriguez, J. M.; Gomez-Herrero, J.; Zamora, F. *Adv. Mater.* **2009**, *21* (20), 2025–2028.
(12) Gritsenko, K. P.; Krasovsky, A. M. *Chem. Rev.* **2003**, *103* (9), 3607–3649.
(13) Inganas, O.; Salaneck, W. R.; Osterholm, J. E.; Laakso, J. *Synth. Met.* **1988**, *22* (4), 395–406.
(14) Kobayashi, S.; Haga, Y. *Synth. Met.* **1997**, *87* (1), 31–36.
(15) Lee, C. H.; Kang, G. W.; Jeon, J. W.; Song, W. J.; Seoul, C. *Thin Solid Films* **2000**, *363* (1−2), 306–309.
(16) D'Almeida, K.; Bernede, J. C.; Marsillac, S.; Godoy, A.; Diaz, F. R. *Synth. Met.* **2001**, *122* (1), 127–129.
(17) Wei, H. Y.; Scudiero, L.; Eilers, H. *Appl. Surf. Sci.* **2009**, *255* (20), 8593–8597.
(18) Yang, H. C.; Shin, T. J.; Yang, L.; Cho, K.; Ryu, C. Y.; Bao, Z. N. *Adv. Funct. Mater.* **2005**, *15* (4), 671–676.
(19) Patricio, P. S. O.; Calado, H. D. R.; de Oliveira, F. A. C.; Righi, A.; Neves, B. R. A.; Silva, G. G.; Cury, L. A. *J. Phys.: Condens. Matter* **2006**, *18* (32), 7529–7542.
(20) Zen, A.; Pflaum, J.; Hirschmann, S.; Zhuang, W.; Jaiser, F.; Asawapirom, U.; Rabe, J. P.; Scherf, U.; Neher, D. *Adv. Funct. Mater.* **2004**, *14* (8), 757–764.
(21) Kline, R. J.; McGehee, M. D.; Kadnikova, E. N.; Liu, J. S.; Frechet, J. M. J.; Toney, M. F. *Macromolecules* **2005**, *38* (8), 3312–3319.
(22) Pretsch, E.; Bühlmann, P.; Badertscher, M., *Structure Determination of Organic Compounds: Tables of Spectral Data*; Springer: New York 2009.
(23) Rico, M.; Orza, J. M.; Morcillo, J. *Spectrochim. Acta* **1965**, *21* (4), 689.
(24) Li, J. Q.; Aoki, K. *J. Electroanal. Chem.* **1998**, *458* (1−2), 155–160.
(25) Singh, R. K.; Kumar, J.; Singh, R.; Kant, R.; Chand, S.; Kumar, V. *Mater. Chem. Phys.* **2007**, *104* (2−3), 390–396.
(26) Chen, T. A.; Wu, X. M.; Rieke, R. D. *J. Am. Chem. Soc.* **1995**, *117* (1), 233–244.
(27) Olinga, T.; Destri, S.; Porzio, W.; Selva, A. *Macromol. Chem. Phys.* **1997**, *198* (4), 1091–1107.
(28) Ferrari, M.; Mucci, A.; Schenetti, L.; Malmusi, L. *Magn. Reson. Chem.* **1995**, *33* (8), 657–663.
(29) Shaw, P. E.; Ruseckas, A.; Samuel, I. D. W. *Adv. Mater.* **2008**, *20* (18), 3516.
(30) Nelson, J., *The Physics of Solar Cells*; Imperial College Press: London, 2003.
(31) Kim, J. S.; Park, Y.; Lee, D. Y.; Lee, J. H.; Park, J. H.; Kim, J. K.; Cho, K. *Adv. Funct. Mater.* **2010**, *20* (4), 540–545.

AM1008985